# 3D Lithography using X-ray Exposure Devices Integrated with Electrostatic and Electrothermal Actuators

**Kwang-Cheol Lee and Seung S. Lee**

*Abstract*— **We present a novel 3D fabrication method with single X-ray process utilizing an X-ray mask in which a micro-actuator is integrated. An X-ray absorber is electroplated on the shuttle mass driven by the integrated micro-actuator during deep X-ray exposures. 3D microstructures are revealed by development kinetics and modulated in-depth dose distribution in resist, usually PMMA. Fabrication of X-ray masks with integrated electrothermal xy-stage and electrostatic actuator is presented along with discussions on PMMA development characteristics. Both devices use 20-μm-thick overhanging single crystal Si as a structural material and fabricated using deep reactive ion etching of silicon-on-insulator wafer, phosphorous diffusion, gold electroplating, and bulk micromachining process. In electrostatic devices, 10-μm-thick gold absorber on 1mm×1mm Si shuttle mass is supported by 10-μm-wide, 1-mm-long suspension beams and oscillated by comb electrodes during X-ray exposures. In electrothermal devices, gold absorber on 1.42 mm diameter shuttle mass is oscillated in x and y directions sequentially by thermal expansion caused by joule heating of the corresponding bent beam actuators. The fundamental frequency and amplitude of the electrostatic devices are around 3.6 kHz and 20μm, respectively, for a dc bias of 100 V and an ac bias of 20 VP-P (peak-peak). Displacements in x and y directions of the electrothermal devices are both around 20 μm at 742 mW input power. S-shaped and conical shaped PMMA microstructures are demonstrated through X-ray experiments with the fabricated devices.**

*Index Terms*— **3D Deep X-ray lithography, electrostatic actuator, LIGA, thermal actuator, xy stage.**

Manuscript received November 15, 2002; revised December 12, 2002.
K. C. Lee, S. S. Lee are with Department of Mechanical Engineering, Pohang University of Science and Technology.
**Email :** kclee@postech.ac.kr **Tel :** +82-54-279-8210
**Fax :** +82-54-279-5899

## I. INTRODUCTION

LIGA is a German acronym stands for deep X-ray lithography (LIthographie), Electroforming (Galvanoformung), and molding (Abformung) process. The LIGA process has been used to fabricate high aspect ratio microstructures with smooth sidewalls due to the X-ray characteristics such as high directionality and high flux. The shape and surface quality of microstructures fabricated with LIGA process are generally determined by the deep X-ray lithography (DXL) step and the control of the cross section of the microstructures or the fabrication of 3D (three-dimensional) microstructures is somehow difficult. Thus, various 3D microfabrication methods with LIGA process including multiple X-ray mask LIGA [1], micro-assembly [2-4], and 3D DXL [5-11] have been conducted to produce 3D microsystems and components.

Multi-level microstructures, microsensors, and

microactuators have been reported using multiple X-ray mask LIGA [1], which uses successive applications of aligned DXL, electroplating, and planarization. 3D microstructures have been demonstrated using serial or batch assembly technique from pre-fabricated single-level LIGA microstructures such as diffusion bonding [2], selective electroplating [3], adhesive bonding [4], and pressure fitting. Protruding 3D shapes such as microlens arrays are also demonstrated using thermal after-treatment of PMMA (Polymethylmethacrylate) cylinders or contactless hot embossing method with cylindrical metal mold insert [12-14].

3D DXL methods such as rotated/inclined DXL [5-6] and moving mask DXL [7-11] have been reported to fabricate elegant 3D microstructures with single DXL step. Complex 3D microstructures have been reported using rotated/inclined DXL in a simple manner [5-6]. However, the cross section of the microstructure is rather limited or the microstructure is limited to solids of revolution. Moreover, the roughness of microstructure often increases because of additional problems such as the existence of the transition region due to the inclined X-rays to the direction of absorber edge, the projection of absorber and blank roughness onto resist, and precision of rotating equipment.

Moving mask DXL [7-11] has unique properties such as ability to produce 3D microstructures with free curved surfaces. Whereas the mask and resist are fixed together in other LIGA processes, the mask and resist move relatively during X-ray exposures in moving mask DXL. At a given depth of resist, the absorbed dose is linearly increased with the exposure time. At a given planar coordinate of resist, the z-directional dose distribution is a function of absorption coefficient of resist. Varying the exposure time at each planar coordinate in resist changes the dose profile in it. In moving mask DXL, the relative motion of X-ray mask realizes the modulation of dose profile in resist. After development at a given time, the shape of resulting microstructure is determined by the resist development characteristics according to the absorbed dose. Some 3D microstructures with slanted sidewalls or free curved surfaces have been reported using moving mask DXL. However, It needs somewhat precious equipments for the motion control of mask.

This paper reports a novel 3D DXL method to fabricate 3D LIGA microstructures with single X-ray process without the necessity of additional system. It utilizes a deep X-ray mask in which a micro-actuator is integrated. Fig. 1 shows a diagram of 3D DXL process using our proposed device, deep X-ray *m*ask with *i*ntegrated micro-*a*ctuator (MIA), compared with that of standard DXL process. Whereas the absorber pattern of conventional deep X-ray mask is formed on the membrane which is fixed to the frame, that of our device is formed on the shuttle mass of integrated micro-actuator. During X-ray exposure, the integrated micro-actuator oscillates the gold (Au) absorber on the shuttle mass to modulate dose profile in resist, typically PMMA. 3D resist microstructures with curved, slanted, and stepped sidewalls are fabricated according to the motion of Au absorber on the shuttle mass, absorber layout, and development kinetics. Here, we present two kinds of the X-ray exposure devices, electrostatically driven 1D MIA and electrothermally driven 2D MIA. Both devices are fabricated using silicon-on-insulator (SOI) wafer, resulting in batch fabricated, overhanging single crystal silicon microstructures as a structural material. Fabrication of the devices and discussions on X-ray experiments will be described.

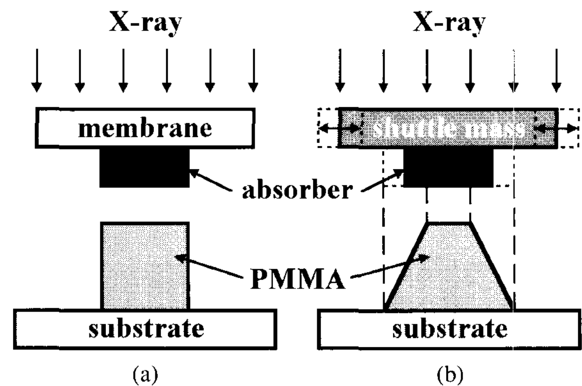


**Fig. 1.** (a) Standard fabrication method of PMMA microstructures with LIGA process compared to (b) 3D fabrication method using a deep X-ray *m*ask with *i*ntegrated micro-*a*ctuator (MIA).

## II. X-RAY DEVICES

### A. *Electrostatically Driven Device*

Fig. 2 shows a schematic view of the device with integrated comb drive actuator and Au absorber on its

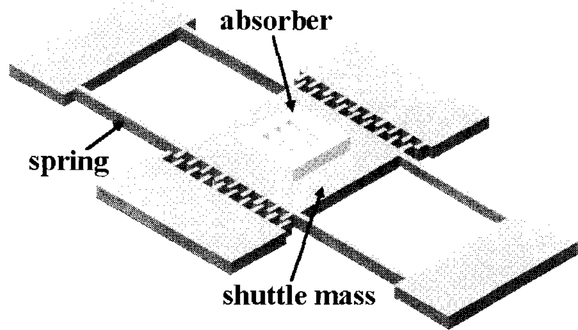


**Fig. 2.** A schematic diagram of electrostatically driven 1D MIA; 20-μm-thick overhanging single crystal silicon microstructures carrying an X-ray absorber on the shuttle mass.

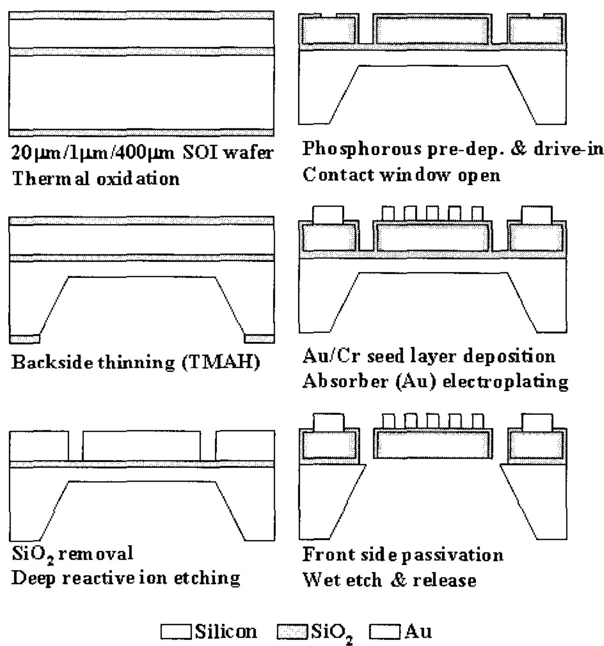


**Fig. 3.** Fabrication process of MIA.

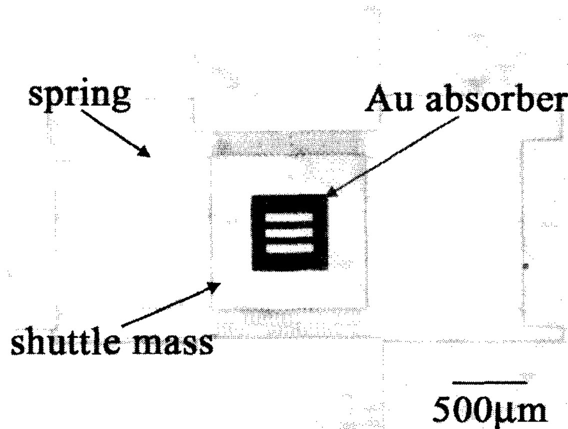


**Fig. 4.** An optical photomicrograph of the fabricated electrostatically driven 1D MIA.

shuttle mass. The integrated comb drive actuator oscillates the shuttle mass at its resonance during X-ray exposures to modify dose profile in resist, usually PMMA. The pads are electrically isolated from the substrate by a buried silicon dioxide layer of silicon-on-insulator (SOI) wafer. The substrate has been etched through, leaving the shuttle mass overhanging a via hole. It eliminates the occurrence of a vertical stiction related to the critical dimensions and a gap between the structure and substrate.

The device is fabricated using deep reactive ion etching (DRIE) of 20-μm-thick device layer of SOI wafer, Au absorber electroplating, phosphorous diffusion, and bulk micromachining process. A 10-μm-thick, 50 μm L/S (line and spaced) Au absorber pattern is electroplated on 20-μm-thick, 1 mm × 1 mm shuttle mass supported by 1-mm-long, 10-μm-wide, and 20-μm-thick four suspension beams. Comb finger width and length are 10 μm and 100 μm, respectively, and finger gap and overlapped length are 10 μm and 30 μm, respectively.

Fig. 3 shows the fabrication process of the electrostatically driven device [15]. The fabrication process starts with a phosphorous-doped, N (100), 1–10 Ω·cm, 20 μm / 1 μm / 400 μm SOI wafer. After the standard cleaning, 0.7-μm-thick $SiO_2$ is grown in wet ambient at 1050 °C as a protection layer to TMAH solution. The backside is anisotropically etched around 300 μm in 20wt.% TMAH at 90 °C to reduce releasing time. After $SiO_2$ removal, the comb drive structure is defined by DRIE (Plasma Therm. Co.) with the 2-μm-thick photoresist mask. After the standard cleaning, phosphorous is diffused by pre-deposition at 1050 °C for 60 minutes with a liquid source, $POCl_3$, followed by drive-in at 1050 °C for 100 minutes in wet ambient. It results in 0.7-μm-thick $SiO_2$ layer for electrical insulation. The sheet resistances before and after drive-in are about 1.7 Ω/sq and 1.1 Ω/sq, respectively. After the contact window opening, 400-nm-thick Au and 50-nm-thick Cr are deposited by thermal evaporation as an electroplating seed layer. Using 20-μm-thick photoresist (AZ9260) mold, the 10-μm-thick Au absorber and pads are electroplated. The Au electroplating is carried out using a cyanide bath at 35 °C with a current density of 2 $mA/cm^2$. The backside is wet etched using 33% KOH

solution at 60 °C using the buried oxide of SOI wafer as a stop layer. During wet etching, the front side is protected by gluing to silicon nitride deposited wafer with black wax. After the buried oxide and seed layer removal, the device is cleaned, IPA rinsed, and dried.

Fig. 4 shows an optical photomicrograph of the fabricated device. The fundamental frequency and the amplitude are around 3.6 kHz and 20 μm, respectively, for a dc bias of 100 V and an ac bias of 20 $V_{P-P}$ (peak to peak).

### B. *Electrothermally Driven Device*

Fig. 5 shows a schematic diagram of the X-ray exposure device with integrated electrothermally driven xy-stage. The device consists of four bent beam actuators crossing each other at the shuttle mass where an Au absorber pattern is electroplated. When a dc or ac current is passed through the x or y bent beam actuators, the shuttle mass is displaced corresponding to the apex motion due to the thermal expansion effects of the bent beams caused by joule heating.

The fabrication process of the electrothermally driven devices is similar with that of the electrostatic devices, resulting in 20-μm-thick overhanging single crystal silicon microstructures isolated by 1-μm-thick buried oxide layer of SOI wafer. The width, length, and bending angle of each bent beam actuator are 20 μm, 1 mm, and 0.1 rad, respectively. The width and length of four suspension beams supporting a 1.42 mm diameter shuttle mass are 10 μm and 1 mm, respectively.

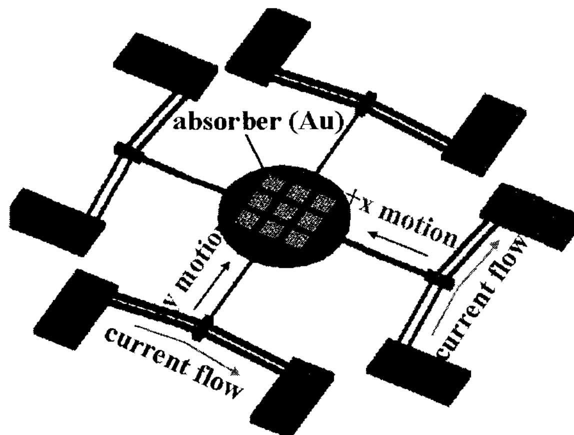


Fig. 5. A schematic diagram of the electrothermally driven 2D MIA; It consists of micro xy-stage driven electrothermally by a set of overhanging single crystal silicon bent beam actuators crossing each other at the shuttle mass carrying an X-ray absorber.

Fig. 6 shows the fabricated electrothermally driven X-ray device mounted on a chip carrier with a close up detail of the overhanging structures (Fig. 6(b)) and a representative quadrilateral Au absorber pattern (Fig.

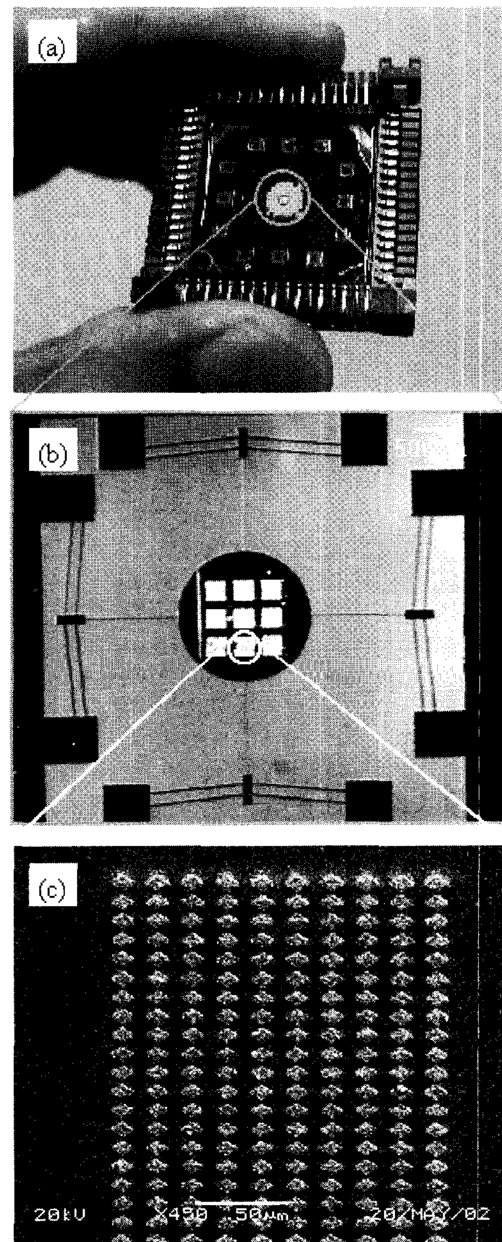


Fig. 6. Photomicrographs of the fabricated electrothermally driven 2D MIA (a) mounted on a chip carrier (b) with a close-up detail of overhanging device and (c) a representative Au absorber array.

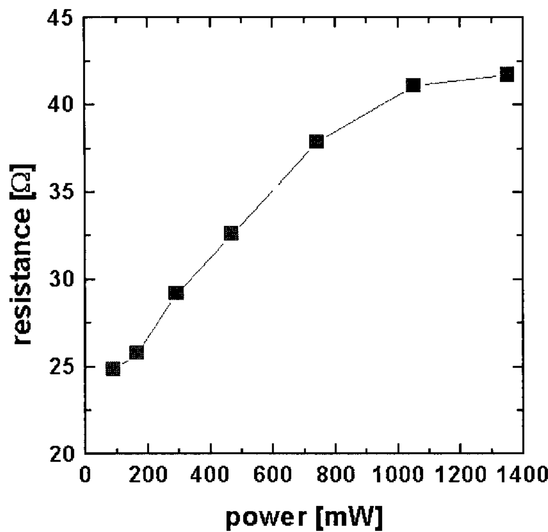


**Fig. 7.** Measured resistance change of the electrothermally driven 2D MIA versus dc input power.

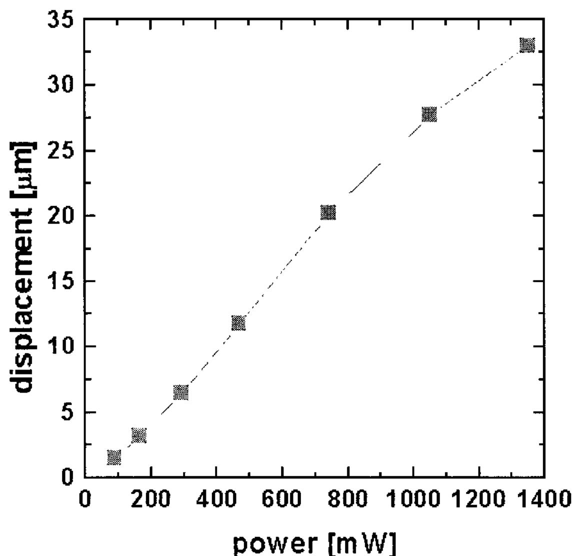


**Fig. 8.** Measured shuttle mass displacement variations of the electrothermally driven 2D MIA versus dc input power.

6(c)). Fig. 7 shows the measured resistance change of the bent beam actuators with respect to the dc input power. The cold resistance at room temperature is around 25 Ω and the difference between each bent beam actuator is not observed. The resistance increases nonlinearly as input power increases, reaching around 42 Ω at 1350 mW input power. At high input powers, the resistance increase is slowed down, showing the device temperature is near the intrinsic temperature of single crystal silicon.

Fig. 8 shows the measured shuttle mass displacement variations according to the dc input power. In these tests, constant current is applied through pads, and the voltage drop is recorded. The displacement variation according to the current is measured using probe station. Measurements are done at room temperature and no extra cooling of the device is carried out. The measured shuttle mass displacements in x and y directions are both around 20 μm at 742 mW input power and increase nonlinearly as the input power increases. The shuttle mass and voltage are oscillated at high input current, which is caused by temperature and resistance variations due to the insufficient heat dissipations through pads.

## III. X-RAY EXPERIMENTS

Deep X-ray exposure experiments with the fabricated devices are carried out at Pohang Light Source (PLS) in Korea, which is operated at 2.5 GeV stored energy and 100-170 mA beam current. Synchrotron X-rays emitted from 1.323 T bending magnet of LIGA beamline at PLS go through two 254-μm-thick Be windows, 400-mm-long He spool, and 130-μm-thick Kapton film and enters 15-m-apart X-ray mask with 12 mrad horizontal divergence. X-ray exposures are performed in air ambient and the devices are cooled down with metal heat sink with water-cooled jacket.

A 20-μm-thick silicon membrane is used as a pre-absorber to reduce the thermal load on the devices during X-ray exposures. Fig. 9 shows the measured PMMA development rate versus absorbed dose at 35 °C GG developer. The linear absorption coefficient and the universal flux distribution integrated over all vertical-opening angles are used for the calculation of absorbed dose distribution in PMMA [16, 17]. After X-ray exposures at doses in the range from 0.2 kJ/cm$^3$ to 4 kJ/cm$^3$, the exposed 2-mm-thick PMMA sheets (Goodfellow) are developed in GG developer (60% diethyleneglycol-buthylether, 20% morpholine, 5% ethanolamine, and 15% deionized water) at 35 °C for a given time, DI rinsed, and $N_2$ dried. The depth change is measured with the surface profiler (DEKTAK 3 ST). From the measured developed depth, development rate as a function of dose value is determined. The threshold dose ($D_o$) of PMMA at 35 °C GG developer is around 1.7 kJ/cm$^3$ as shown in Fig. 9. The development rate increases linearly as the dose increases above 2 kJ/cm$^3$

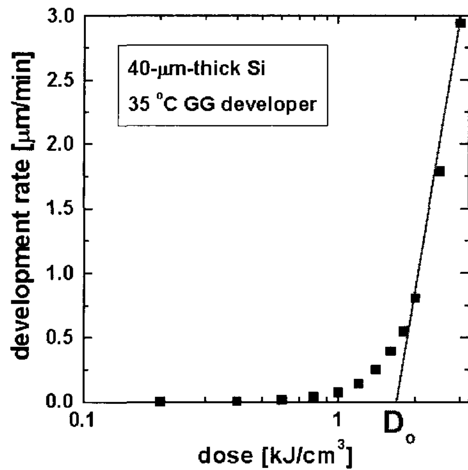


**Fig. 9.** Measured PMMA development rate versus absorbed dose at 35 °C GG developer.

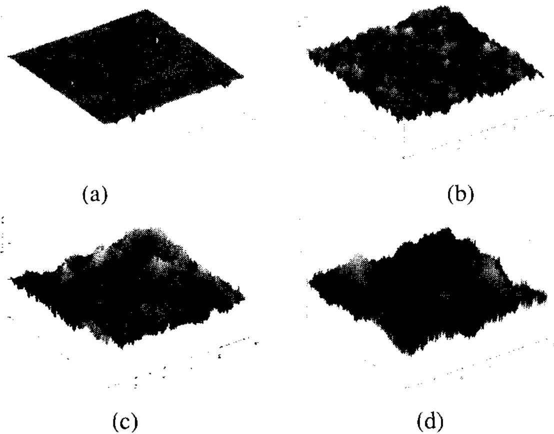


**Fig. 10.** Representative 10 μm × 10 μm AFM micrographs of (a) the pristine 2-mm-thick PMMA sheet (Goodfellow Inc.) and of the exposed PMMA with absorbed dose of (b) 1 kJ/cm$^3$, (c) 2 kJ/cm$^3$, and (d) 3 kJ/cm$^3$ and 35 °C GG development.

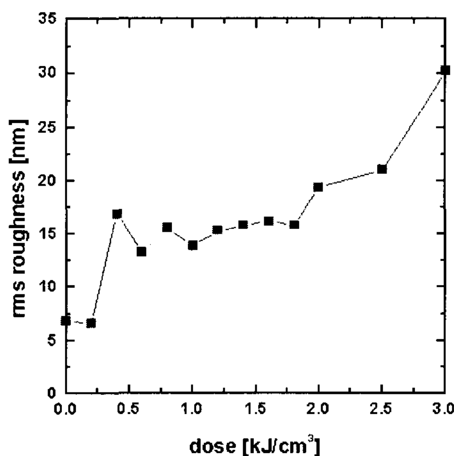


**Fig. 11.** PMMA rms (root mean square) surface roughness after 35 °C GG development versus absorbed dose measured by atomic force microscope.

and increases nonlinearly in the transition region below 2 kJ/cm$^3$.

The 3D fabrication method with fabricated X-ray devices relies on the modulated dose profile according to the absorber trajectories and the development behavior of the exposed resist. Thus, doses in fabricated resist microstructures are higher than doses in fabricated resist microstructures with the conventional LIGA process, which are usually below 100 J/cm$^3$. As the absorbed dose in PMMA increases, the surface roughness of PMMA microstructures could increase and the cracks due to the gas generation within PMMA might be occurred. Fig. 10 shows representative 10 μm × 10 μm AFM images of PMMA surfaces after exposures at doses of 1 kJ/cm$^3$, 2 kJ/cm$^3$, and 3 kJ/cm$^3$, respectively, and after 35 °C GG development along with that of pristine 2-mm-thick PMMA sheet. Fig. 11 shows the PMMA rms (root mean square) surface roughness variations versus absorbed dose. The rms surface roughness at doses in the range of 1 kJ/cm$^3$ and 2 kJ/cm$^3$ is around 15-20 nm compared to 6 nm of pristine PMMA. The surface roughness increases as dose increases showing near 30 nm in rms at 3 kJ/cm$^3$ dose. In order to reduce the surface roughness of PMMA microstructures, we have used low doses in the range of 1–2 kJ/cm$^3$ for the fabrication of microstructures compared to the conventional LIGA process that uses doses above 3 kJ/cm$^3$.

Fig. 12 shows the fabricated PMMA microstructure with the electrostatic devices for 1.6 kJ/cm$^3$ surface dose and GG development at 35 °C for 40 minutes. The depth of PMMA microstructure is around 15.4 μm and the development rate is around $0.38\,\mu m/\text{min}$. Inset in Fig. 12(b) shows the calculated cross-sectional profile from the development curve and calculated in-depth dose distribution. Contrary to the calculated convex cross section, the fabricated PMMA microstructure shows convex and concave (S-shaped) cross section with a turning point near 1 kJ/cm$^3$. The deviation of the fabricated cross section from the calculated profile is reported partly due to an intermittent exposure effect [10] and can be resolved by adapting the absorber layout or actuator displacement pattern.

Fig. 13 shows conical and tapered PMMA microstructure arrays fabricated with electrothermal devices. The devices are oscillated in x and y directions

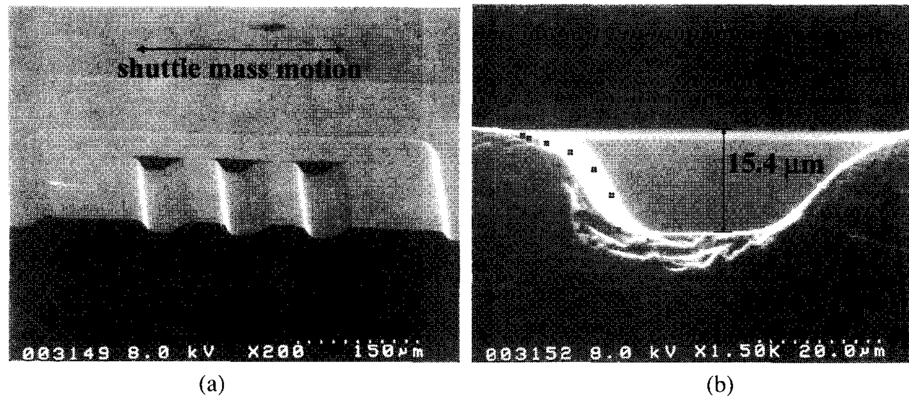


(a) (b)

**Fig. 12.** SEM photomicrographs of PMMA microstructure fabricated with electrostatic devices: inset in (b) shows the calculated cross-sectional profile.

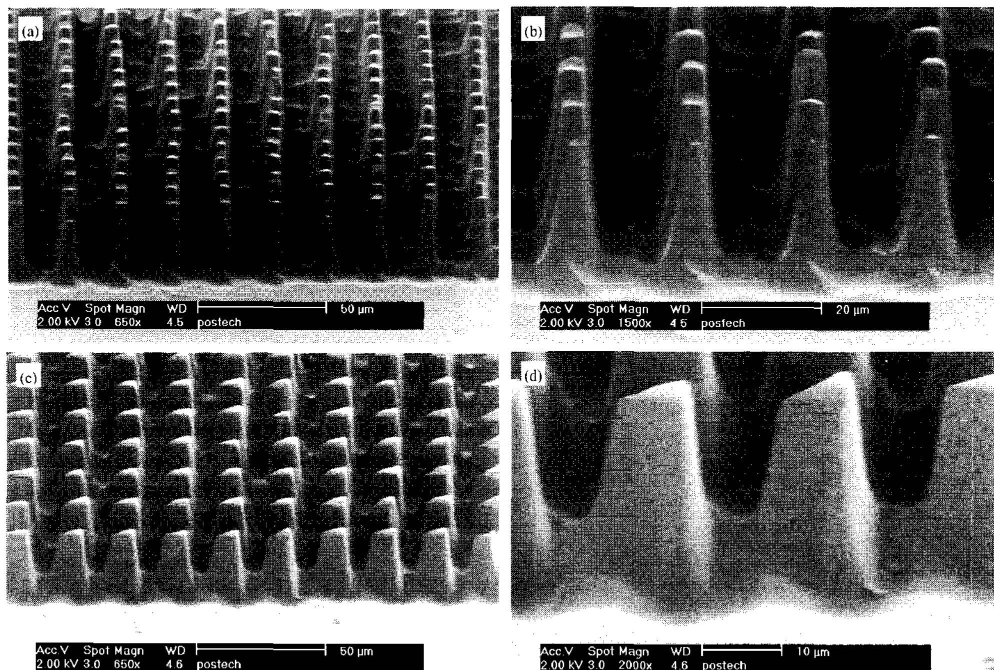


**Fig. 13.** SEM photomicrographs of PMMA microstructure arrays fabricated with electrothermal devices.

sequentially at 1 *Hz* sinusoidal wave during exposures at 1.6 kJ/cm$^3$ surface dose and the exposed PMMA sheets are developed at 35 °C GG developer.

## IV. Conclusions

We presented a novel 3D fabrication method with single X-ray process utilizing a deep X-ray *m*ask with *i*ntegrated *a*ctuator (MIA). Two kinds of the X-ray exposure devices, electrostatically driven 1D and electrothermally driven 2D MIA, are fabricated and tested. Both devices are fabricated using a SOI wafer with 20-μm-thick device layer, resulting overhanging single crystal silicon microstructures. The fundamental frequency and amplitude of the electrostatic devices are around 3.6 kHz and 20 μm, respectively, for a dc bias 100 V and an ac bias of 20 $V_{P-P}$ (peak to peak). Displacements in x and y directions of the electrothermal devices are both around 20 μm at 742 mW input power. S-shaped and conical shaped PMMA microstructures are demonstrated through X-ray experiments with the fabricated devices.

## ACKNOWLEDGEMENTS

This research, under the contract project code MS-02-338-01, has been supported by the Intelligent Microsystem Center (IMC: http://www.microsystem.re.kr), which carries out one of the 21st century's Frontier R & D Projects sponsored by the Korea Ministry of Science & Technology.

## REFERENCES

[1] H. Guckel, "High-aspect-ratio micromachining via deep X-ray lithography," *Proc. of the IEEE*, 86, pp. 1586-1593, 1998.

[2] T. R. Christenson and D. T. Schmale, "A batch wafer scale LIGA assembly and packaging technique via diffusion bonding," in *Technical Digest of the 12th IEEE International Conference on Microelectromechanical Systems (MEMS'99)*, Orlando, FL, USA, 17-21 January 1999, pp. 476-481.

[3] L.-W. Pan and L. Lin, "Batch transfer of LIGA microstructures by selective electroplating and bonding," *J. of Microelectromech. Syst.*, 10, pp. 25-32, 2001.

[4] D. Maas, B. Büstgens, J. Fahrenberg, W. Keller, P. Ruther, W. K. Schomburg, and D. Seidel, "Fabrication of microcomponents using adhesive bonding techniques," in *Technical Digest of the 9th IEEE International Conference on Microelectromechanical Systems (MEMS'96)*, San Diego, CA, USA, 11-15 February 1996, pp. 331-336.

[5] V. White, C. Herdey, D. D. Denton, and J. Song, "X-ray fabrication of nonorthogonal structures using "surface" masks," *J. Vac. Sci. Technol. B*, 15, pp. 2514-2516, 1997.

[6] W. Ehrfeld and A. Schmidt, "Recent developments in deep X-ray lithography," *J. Vac. Sci. Technol. B*, 16, pp. 3526-3534, 1998.

[7] A. D. Feinerman, R. E. Lajos, V. White, and D. D. Denton, "X-ray lathe: an X-ray lithographic exposure tool for nonplanar objects," *J. of Microelectromech. Syst.*, 5, pp. 250-255, 1996.

[8] T. Katoh, N. Nishi, M. Fukugawa, H. Ueno, and S. Sugiyama, "Direct writing for three-dimensional microfabrication using synchrotron radiation etching," *Sensors Actuators A*, 89, pp. 10-15, 2001.

[9] S. Sugiyama and H. Ueno, "Novel shaped microstructures processed by deep X-ray lithography," in *Technical Digest of the 2001 International Conference on Solid State Sensors and Actuator (Transducers'01)*, Munich, Germany, 10-14 June 2001, pp. 1574-1577.

[10] O. Tabata, N. Matsuzuka, T. Yamaji, and H. You, "Fabrication of 3-dimensional microstructures using moving mask deep X-ray lithography ($M^2$DXL)," in *Technical Digest of the 14th IEEE International Conference on Microelectromechanical Systems (MEMS'01)*, Interlaken, Switzerland, 21-25 January 2001, pp. 94-97.

[11] O. Tabata, N. Matsuzuka, T. Yamaji, S. Uemura, and K. Yamamoto, "3D microfabrication by moving mask deep X-ray lithography ($M^2$DXL) with multiple stages," in *Technical Digest of the 15th IEEE International Conference on Microelectromechanical Systems (MEMS'02)*, Las Vegas, NV, USA, 20-24 January 2002, pp. 180-183.

[12] P. Ruther, B. Gerlach, J. Göttert, M. Ilie, J. Mohr, A. Müller, and C. Oßmann, "Fabrication and characterization of microlenses realized by a modified LIGA process," *Pure. Appl. Opt.*, 6, pp. 643-653, 1997.

[13] J. Schulze, W. Ehrfeld, J. Hoßfeld, M. Klaus, M. Kufner, S. Kufner, H. Müller, and A. Picard, "Parallel optical interconnections using self-adjusting microlenses on injection molded ferrules made by LIGA technique," in *Proc. SPIE Vol. 3737*, 1999, pp. 562-571.

[14] L.-W. Pan, L. Lin, and J. Ni, "Cylindrical plastic lens array fabricated by a micro intrusion process," in *Technical Digest of the 12th IEEE International Conference on Microelectromechanical Systems (MEMS'99)*, Orlando, FL, USA, 17-21 January 1999, pp. 217-221.

[15] K.-C. Lee and Seung S. Lee, "Deep X-ray mask with integrated actuator for 3D microfabrication," in *Proc. Pacific Rim Workshop on Transducers and Micro/Nano Technologies*, Xiamen, China, 22-24 July 2002, pp. 71-74.

[16] Y. Cheng, N.-Y. Kuo, and C. H. Su, "Dose distribution of synchrotron X-ray penetrating materials of low atomic numbers," *Rev. Sci. Instrum.*, 68, pp. 180-183, 1997.

[17] H. Winick, *Synchrotron radiation research*, H. Winick and S. Doniach, Ed., New York: Plenum Press, 1980, Ch. 2, pp. 11-25.

**Kwang-Cheol Lee** received the B.S. degree in physics from Korea Advanced Institute of Science and Technology, Korea, in 1990, and the M.S. degree in physics from Pohang University of Science and Technology, Korea, in 1992. He is currently working toward the Ph.D. degree in mechanical engineering at Pohang University of Science and Technology, Korea.

From 1992 to 1999, he worked in the area of process development and microsensors at Research Institute of Industrial Science and Technology, Korea. His research

interests include microactuators, microsensors, and LIGA process. Currently, he is concentrating on 3D deep X-ray lithography using mask with integrated microactuator and LIGA process.

**Seung S. Lee** received the B.S. degree from Seoul National University, Korea, in 1984, and the M.S. degree in Mechanical Engineering from University of California, Berkely, CA, in 1989. After his M.S. degree, he joined the Berkely Sensor and Actuator Center and got Ph.D. there in 1995. After 1 year at Samsung Advanced Institute of Technology in Kiheung, Korea, he joined the faculty of the Department of Mechanical Engineering in Pohang University of Science and Technology, Pohang, Korea, in 1997. He is an associate professor now.
His research interests include all aspects of design, fabrication, and analysis of MEMS, bio-MEMS, and LIGA.